Published in final edited form as:
Biochemistry. 2009 June 16; 48(23): 5446–5455. doi:10.1021/bi900186u.

Biosynthesis of UDP-GlcNAc(3NAc)A by WbpB, WbpE, and WbpD: Enzymes in the Wbp Pathway Responsible for O-antigen Assembly in *Pseudomonas aeruginosa* PAO1[†]

Angelyn Larkin[‡] and **Barbara Imperiali**[‡,§,*]

‡*Department of Chemistry, Massachusetts Institute of Technology, 77 Massachusetts Avenue, Cambridge, MA 02139*

§*Department of Biology, Massachusetts Institute of Technology, 77 Massachusetts Avenue, Cambridge, MA 02139*

Abstract

The B-band O-antigen of the lipopolysaccharide found in the opportunistic pathogen *Pseudomonas aeruginosa* PAO1 (serotype O5) comprises a repeating trisaccharide unit that is critical for virulence and protection from host defense systems. One of the carbohydrates in this repeating unit, the rare diacetylated aminuronic acid derivative 2,3-diacetamido-2,3-dideoxy-*β*-D-mannuronic acid (ManNAc(3NAc)A), is thought to be produced by five enzymes (WbpA, WbpB, WbpE, WbpD and WbpI) in a stepwise manner starting from UDP-GlcNAc. Although the genes responsible for the biosynthesis of this sugar are known, only two of the five encoded proteins (WbpA and WbpI) have been thoroughly investigated. In this report, we describe the cloning, overexpression, purification and biochemical characterization of the three central enzymes in this pathway, WbpB, WbpE, and WbpD. Using a combination of capillary electrophoresis, RP-HPLC and NMR spectroscopy, we show that WbpB and WbpE are a dehydrogenase/aminotransferase pair that converts UDP-GlcNAcA to UDP-GlcNAc($3NH_2$)A in a coupled reaction via a unique NAD^+ recycling pathway. In addition, we confirm that WbpD catalyzes the acetylation of UDP-GlcNAc($3NH_2$)A to give UDP-GlcNAc(3NAc)A. Notably, WbpA, WbpB, WbpE, WbpD and WbpI can be combined in vitro to generate UDP-ManNAc(3NAc)A in a single reaction vessel, thereby providing supplies of this complex glycosyl donor for future studies of LPS assembly. This work completes the biochemical characterization of the enzymes in this pathway and provides novel targets for potential therapeutics to combat infections with drug resistant *P. aeruginosa* strains.

The gram-negative pathogen *Pseudomonas aeruginosa* is a versatile organism responsible for infection in immunocompromised individuals (1). It is a major source of hospital-acquired pneumonia and bacteremia, causes severe inflammation and pulmonary failure in cystic fibrosis patients, and has emerged as a serious public health threat (2-5). Effective treatment of *P. aeruginosa* infection has proved challenging due to the strong inherent resistance of the organism to traditional antibiotics and the increasing emergence of multi-drug resistant strains (6-8). While several vaccines for *P. aeruginosa* have been described, none have thus far achieved clinical success (9).

[†]This work was supported by a grant from National Institutes of Health (GM039334 to B.I.).

*To whom correspondence should be addressed: Massachusetts Institute of Technology, 77 Massachusetts Avenue, Cambridge, MA 02139. Phone: (617) 253-1838; Fax: (617) 452-2419; Email: E-mail: imper@mit.edu.

SUPPORTING INFORMATION AVAILABLE Table of constructs and oligonucleotides used in this study, as well as full ^1H, ^{13}C and COSY NMR spectra of UDP-GlcNAc($3NH_2$)A and UDP-GlcNAc(3NAc)A. This material is available free of charge via the Internet at http://pubs.acs.org.

One of the major factors affecting the virulence of *P. aeruginosa* is the composition of unique carbohydrates that makes up the lipopolysaccharide (LPS)[1] (4,10). Localized in the exterior leaflet of the outer membrane of the organism, the *P. aeruginosa* LPS is composed of three distinct regions: lipid A, which anchors the structure to the membrane, a core oligosaccharide, and the O-antigen, a strand of monosaccharides that is further classified as either A-band or B-band (Figure 1) (11-13). Unlike the A-band O-antigen, which is a homopolymer of D-rhamnose, the B-band O-antigen is structurally complex and can vary between strains; this diversity serves as the basis for serological classification of particular strains of the organism (14-16). In addition, the B-band O-antigen has been shown to play a critical role in host colonization and provides resistance to both serum sensitivity and phagocytosis (12,17,18). In *P. aeruginosa* PAO1 (serotype O5), the B-band O-antigen is composed of repeating units of a trisaccharide containing 2-acetamido-3-acetamidino-2,3-dideoxy-*β*-D-mannuronic acid (ManNAc(3NAm)A), 2,3-diacetamido-2,3-dideoxy-*β*-D-mannuronic acid (ManNAc(3NAc)A), and *N*-acetyl-*α*-D-fucosamine (Fuc2NAc) (19). Interestingly, it has been shown that while all three of these carbohydrates are derived from a common precursor, UDP-GlcNAc, the biosynthesis of each involves a distinct set of genes (20).

A combination of genetic and biochemical analyses have resulted in the proposal that the UDP-activated form of the second sugar in the B-band O-antigen, UDP-ManNAc(3NAc)A, is the product of genes in the Wbp pathway (Figure 2). The enzymes encoded by these genes are thought to convert UDP-GlcNAc to UDP-ManNAc(3NAc)A in a stepwise fashion, followed by the transfer of the ManNAc(3NAc)A moiety onto an undecaprenyl carrier by the putative glycosyltransferase WbpH (12,21). The biosynthetic pathway begins with WbpA, previously shown to catalyze the C6-oxidation of UDP-GlcNAc to give the corresponding UDP-*N*-acetyl-D-glucosaminuronic acid (UDP-GlcNAcA) (22). It is then hypothesized that the C3-dehydrogenase WbpB, aminotransferase WbpE, and acetyltransferase WbpD sequentially convert UDP-GlcNAcA into UDP-2,3-diacetamido-2,3-dideoxy-D-glucuronic acid (UDP-GlcNAc(3NAc)A). Finally, the C2-epimerase WbpI modifies UDP-GlcNAc(3NAc)A to give the final UDP-ManNAc(3NAc)A (23). Genetic mutants of *P. aeruginosa* in which *wbpA*, *wbpB*, *wbpE*, *wbpD*, and *wbpI* have been deleted lack the B-band O-antigen, thus highlighting their critical importance to pathogenicity (21,24,25).

Herein, we present the cloning, overexpression, and in vitro characterization of the three central enzymes in this pathway, WbpB, WbpE, and WbpD, and demonstrate that they are responsible for the biosynthesis of UDP-GlcNAc(3NAc)A. We also identify a novel NAD^+ recycling mechanism which requires the coupling of WbpB and WbpE, the dehydrogenase and aminotransferase, to give the WbpE product UDP-GlcNAc($3NH_2$)A. Furthermore, WbpB, WbpE and WbpD can be used in conjunction with WbpA and WbpI to convert UDP-GlcNAc to UDP-ManNAc(3NAc)A in a one-pot reaction. This work completes the biochemical characterization of the UDP-ManNAc(3NAc)A biosynthesis pathway in *P. aeruginosa* and provides, for the first time, a straightforward synthetic route to multimilligram quantities (>

[1]Abbreviations: AcCoA, acetyl-coenzyme A; Bicine, *N*,*N*-Bis(2-hydroxyethyl)glycine; CE, capillary electrophoresis; CoA, coenzyme A; CHES, 2-(*N*-cyclohexylamino)ethanesulfonic acid; COSY, correlation spectroscopy; ESI, electrospray ionization; IPTG, isopropyl β-D-1-thiogalactopyranoside; HEPES, 4-(2-hydroxyethyl)-1-piperazineethanesulfonic acid; HMBC, heteronuclear multiple quantum coherence; HSQC, heteronuclear single quantum coherence; 2-HG, 2-hydroxyglutarate; α-KG, α-ketoglutarate; LPS, lipopolysaccharide; MES, 4-morpholineethanesulfonic acid; MWCO, molecular weight cutoff; NAD^+, nicotinamide adenine dinucleotide; Ni-NTA, nickel nitrilotriacetic acid; NMR, nuclear magnetic resonance; OPD, *o*-phenylenediamine; PLP, pyridoxal 5′-phosphate; RP-HPLC, reversed-phase high-performance liquid chromatography; SDS-PAGE, sodium dodecyl sulfate polyacrylamide gel electrophoresis; TEAB, triethylammonium bicarbonate; TLC, thin-layer chromatography; UDP, uridine 5′-diphosphate; UDP-GlcA, UDP-D-glucuronic acid; UDP-GlcNAc, UDP-*N*-acetyl-D-glucosamine; UDP-GlcNAcA, UDP-*N*-acetyl-D-glucosaminuronic acid; UDP-GlcNAc(3keto)A, UDP-2-acetamido-2-deoxy-3-oxo-D-glucuronic acid; UDP-GlcNAc($3NH_2$)A, UDP-2-acetamido-3-amino-2,3-dideoxy-D-glucuronic acid; UDP-GlcNAc(3NAc)A, UDP-2,3-diacetamido-2,3-dideoxy-D-glucuronic acid; UDP-ManNAc(3NAc)A, UDP-2,3-diacetamido-2,3-dideoxy-D-mannuronic acid.

20 mg) of the rare nucleotide sugar UDP-GlcNAc(3NAc)A, a critical intermediate for future studies of LPS assembly.

EXPERIMENTAL PROCEDURES

Cloning of wbpB, wbpE, and wbpD

The *wbpB*, *wbpE*, and *wbpD* genes were amplified by the polymerase chain reaction from *Pseudomonas aeruginosa* PAO1-LAC genomic DNA (ATCC) using Pfu Turbo polymerase (Stratagene) and the oligonucleotides described in the Supporting Information (Table S1). The resulting PCR products containing both BamHI and XhoI restriction sites were digested and cloned into the same sites of the pET24a(+) vector (Novagen) via standard molecular biology techniques. The final gene products encoded proteins with an N-terminal T7-tag and a C-terminal His_6-tag. Sequencing of all three constructs was performed by the MIT CCR Biopolymers Laboratory (Cambridge, MA).

Overexpression of WbpB, WbpE, and WbpD

The pET24a(+) plasmids containing either *wbpB*, *wbpE*, or *wbpD* were transformed into *E. coli* BL21-CodonPlus(DE3) RIL competent cells (Stratagene) using both kanamycin (50 μg/mL) and chloramphenicol (30 μg/mL) for selection. For overexpression, 1 L of Luria-Bertani media supplemented with kanamycin and chloramphenicol was inoculated with a 5 mL starter culture and allowed to incubate at 37 °C while shaking until an optical density (600 nm) of 0.6-0.8 was achieved. The cultures were then cooled to 16 °C and protein expression was induced by the addition of IPTG (1 mM). After 16 hours, the cells were harvested by centrifugation (5,000 × *g*) and the resultant cell pellets were stored at −80 °C until needed.

Purification of WbpB, WbpE, and WbpD

All steps were performed at 4 °C. The cell pellets from a 1 L culture were thawed and resuspended in 50 mL cold lysis buffer (50 mM HEPES, pH 8.0/300 mM NaCl/10 mM imidazole) and disrupted by ultrasonication on ice. The cell lysate was then cleared of unbroken cells, cellular debris, and membranes by centrifugation (145,000 × *g*) for 65 minutes. The resulting supernatant was incubated with Ni-NTA agarose resin (Qiagen) for 2 hours with gentle rocking and subsequently poured into a fritted PolyPrep column (BioRad) to collect the resin. The resin was washed (50 mM HEPES, pH 8.0/300 mM NaCl/25 mM imidazole) and the protein eluted (50 mM HEPES, pH 8.0/300 mM NaCl/250 mM imidazole). Fractions containing the desired product were combined and dialyzed (50 mM HEPES, pH 8.0/100 mM NaCl) to remove the imidazole and lower the salt concentration. Proteins were stored at either −20 °C (WbpB, WbpE) or 4 °C (WbpD) after the removal of precipitate by filtration and addition of glycerol to a final concentration of 25%. Protein purity was measured by SDS-PAGE, and protein identity was confirmed by Western blot analysis using both Anti-T7 (Novagen) and Anti-His_4 (Qiagen) antibodies. Protein concentration was determined by either the Micro BCA kit (Pierce) or UV absorbance using the following extinction coefficients at 280 nm: WbpB (38,150 $M^{-1}cm^{-1}$), WbpE (20,040 $M^{-1}cm^{-1}$), WbpD (22,340 $M^{-1}cm^{-1}$).

Synthesis of UDP-GlcNAcA

UDP-GlcNAcA was prepared via oxidation of UDP-GlcNAc as previously described (26). After filtration to remove the Pt catalyst, the desired product was purified from the UDP-GlcNAc starting material using a 5 mL HiTrap Q FF anion exchange column (GE Healthcare), eluting with a linear gradient of 0-0.5 M NH_4HCO_3 over 250 mL. Fractions containing UDP-GlcNAcA were combined, freeze-dried, and resuspended in H_2O for further purification using a Synergi C_{18} Hydro preparatory RP-HPLC column (4 μm, 80 Å, 250 × 21.2 mm, Phenomenex) for removal of impurities and salt. The HPLC column was equilibrated with 50 mM

triethylammonium bicarbonate (TEAB, pH 7.1) and, after loading, the product was eluted using a gradient of 0-50% CH_3CN over 30 minutes. The desired UDP-GlcNAcA was characterized by ESI-MS and ^1H, ^{13}C, and ^{31}P NMR spectroscopy, and the resulting data were found to match previously published values (26).

Functional Characterization of WbpB/WbpE and WbpD

WbpB/WbpE coupled reactions to produce UDP-GlcNAc($3NH_2$)A contained 2.5 μg of each enzyme, 1 mM UDP-GlcNAcA, 0.2 mM NAD^+, 25 mM L-glutamate, 0.1 μM PLP, 2.5 mM DTT, 2 mM $MgCl_2$, and 50 mM HEPES (pH 8.0) in a total reaction volume of 30 μL. Reactions were incubated at 30 °C for 8 hours prior to analysis by capillary electrophoresis. For ^{15}N-labeling of UDP-GlcNAc($3NH_2$)A, ^{15}N-L-glutamate was utilized in the place of L-glutamate. For synthesis of UDP-GlcNAc(3NAc)A by WbpD, reactions contained 1 μg of enzyme, 1.0 mM UDP-GlcNAc($3NH_2$)A, 1.0 mM AcCoA, and 50 mM HEPES (pH 7.0). These reactions were incubated at 30 °C for 2 hours prior to CE analysis. To incorporate [^3H] into UDP-GlcNAc (3NAc)A, [^3H]-AcCoA was used in the place of AcCoA. For determination of pH optima, reactions included 50 mM MES (pH 5.5, 6.0, 6.5), 50 mM HEPES (pH 7.0, 7.5 8.0), 50 mM Bicine (pH 8.5), or 50 mM CHES (pH 9.0, 9.5, 10.0). To study temperature requirements, reactions were incubated at 4, 16, 25, 30, 37, 42, and 65 °C for the appropriate time. In all cases, the presence of product was confirmed by the addition of starting material into reaction mixtures and the observation of a new peak by CE.

Analysis of Reaction Products by Capillary Electrophoresis

CE was performed using a P/ACE MDQ system (Beckman Coulter) equipped with a UV detector. Bare silica capillary (75 μm × 80 cm) was utilized with detection at 72 cm and 25 mM sodium tetraborate (pH 9.5) as the running buffer. Prior to each run, the capillary was conditioned sequentially with 0.1 M NaOH, H_2O, and running buffer for 2 minutes. Samples were introduced to the capillary by pressure injection for 15 seconds at 30 mbar and separation was performed at 22 kV and monitored by UV absorbance at 254 nm. In general, samples were prepared by filtration with a 5K MWCO membrane (Millipore) and diluted (2x) with H_2O. Manual peak integration was carried out using Beckman 32 Karat software suite.

Purification and Characterization of WbpB/WbpE and WbpD Reaction Products

A large-scale WbpB/WbpE coupled reaction contained 4.5 mg of each enzyme, 0.75 mM UDP-GlcNAcA, 0.2 mM NAD^+, 25 mM L-glutamate, 0.1 mM PLP, 50 mM HEPES (pH 8.0), 2.5 mM DTT, and 2 mM $MgCl_2$ in a total volume of 50 mL. Reactions were incubated at 30 °C for 24 hours, during which time the progress of the reaction was monitored by CE. Protein was removed from the mixture by filtration and the resulting filtrate was frozen and lyophilized. The crude mixture was resuspended in H_2O and loaded onto a Synergi C_{18} Hydro preparatory RP-HPLC column equilibrated with 50 mM TEAB (pH 7.1). The UDP-GlcNAc($3NH_2$)A product was eluted with a linear gradient of 0-50% CH_3CN over 65 minutes. Preparative-scale WbpD reactions contained 1.5 mg enzyme, 0.75 mM UDP-GlcNAc($3NH_2$)A, 0.75 mM AcCoA and 50 mM HEPES (pH 7.0) in a final volume of 7 mL. The reactions were incubated at 30 °C for 2 hours. The crude reaction mixture was filtered, lyophilized, and purified as described for UDP-GlcNAc($3NH_2$)A. Quantification of the products was carried out using the molar extinction coefficient of uridine (ε_{262nm} = 10,000 $M^{-1}cm^{-1}$). NMR spectra were acquired using either a Bruker 600 MHz spectrometer equipped with a 5 mm inverse cryoprobe or a Varian Inova 500 MHz spectrometer equipped with a 5 mm inverse broadband gradient probe. The UDP-sugar to be analyzed was dissolved in 150 μL D_2O and freeze-dried several times prior to NMR analysis using a Shigemi tube (Shigemi Corp). The HOD signal at 4.80 ppm was used as an internal reference for ^1H analysis and the $(CH_3\underline{C}H_2)_3N$ signal of triethylamine at 47.19 ppm was utilized for ^{13}C observation. An external reference of 85%

H_3PO_4 was employed for ^{31}P NMR. High-resolution ESI-MS was performed by Department of Chemistry Instrumentation Facility at MIT (Cambridge, MA).

Verification of α-Ketoglutarate as the Required Oxidant for WbpB Function

To identify if α-KG was the required oxidant for NAD^+ regeneration by WbpB, a reaction containing 0.75 mM UDP-GlcNAcA, 50 mM HEPES (pH 8.0), 10 mM α-KG, and 5 μg WbpB in a total volume of 60 uL was assembled. The reaction was incubated at 30 °C for two hours prior to analysis by CE. After removal of the enzyme by filtration, thin-layer chromatography was utilized to observe the formation of 2-hydroxyglutarate (2-HG) in the crude reaction mixture. Samples were run on silica gel 60 F_{254} plates (EMD Biosciences) in a butanol/formic acid/H_2O mixture (8:3:2), air-dried, and developed either directly with dinitrophenylhydrazine or heated at 120 °C and stained with bromocresol green (27).

In order to confirm the consumption of α-KG by WbpB, a similar reaction containing 0.75 mM UDP-GlcNAcA, 50 mM HEPES (pH 8.0), 2 mM α-KG and 2.5 μg WbpB in a volume of 250 μL was prepared. Aliquots (25 μL) were removed from the reaction at several time points, quenched in 225 μL 1 M H_3PO_4, and split into two 125 μL fractions. A solution of *o*-phenylenediamine (OPD, 30 quenched in μL), a specific labeling agent for α-keto acids (28, 29), was then added to one 125 μL fraction, while the other was kept as an unlabeled control. The freshly prepared OPD solution consisted of 1 mg OPD in 1 mL H_3PO_4 (adjusted to pH 2 with 1 M NaOH) and 2.5 μL β-mercaptoethanol. All OPD-labeled samples were boiled for 5 minutes and then cooled to room temperature prior to analysis by UV absorbance at 340 nm. The absorbance measurements of the unlabeled fractions were subtracted from readings of the corresponding OPD-labeled samples; the resulting data represent the average of three experiments.

Identification of the Cofactor Bound to WbpB

In order to identify whether WbpB utilizes NAD^+ or $NADP^+$ as the preferred tightly bound cofactor, procedures previously outlined were employed with slight modification (30,31). Briefly, 500 μg of purified WbpB (in 2 mL 50 mM HEPES, pH 8.0/100 mM NaCl) was precipitated by incubation with 10 μL 60% aqueous $HClO_4$ on ice for 20 minutes followed by centrifugation (7,000 × *g*). The supernatant was removed and the precipitate washed twice with 250 mL cold HEPES/NaCl buffer and spun down. The combined supernatants were neutralized with saturated $NaHCO_3$ and freeze-dried. The dried extract was then resuspended in 300 μL alcohol dehydrogenase buffer (45 mM glycine/75 mM sodium pyrophosphate, pH 9.0/170 mM EtOH) and transferred to a cuvette. NAD^+-specific alcohol dehydrogenase (10 μg, 445 units/mg, Sigma-Aldrich) was added and NADH formation was monitored by UV absorbance at 340 nm. After 10 minutes, $NADP^+$ (20 μM) was added to assess cofactor specificity and 5 minutes later, NAD^+ (20 μM) was introduced as a control for enzyme activity. The same procedure was performed using the $NADP^+$-specific isocitric dehydrogenase (20 μg, 95 units/mg, Sigma-Aldrich), using a solution containing 6 mM isocitric acid and 50 mM HEPES (pH 7.0) to dissolve the WbpB extract (30).

Determination of Kinetic Parameters of WbpD

For determination of UDP-GlcNAc($3NH_2$)A kinetics, all reactions contained 0.5 ng of freshly purified WbpD, 1.5 mM AcCoA, 50 mM HEPES (pH 7.0), 5 μg bovine serum albumin as a carrier protein, and varying concentrations of UDP-GlcNAc($3NH_2$)A (0.015-1.5 mM) in a total reaction volume of 30 μL. The reactions were incubated at 30 °C for 45 minutes, boiled for 2 minutes to inactivate the enzyme, and analyzed by CE to determine the amount of UDP-GlcNAc(3NAc)A produced. The kinetic parameters were determined from linear regression analysis and are the average of two experiments.

One-Pot Synthesis of UDP-ManNAc(3NAc)A

In order to synthesize UDP-ManNAc(3NAc)A in a one-pot process, 50 μg each of WbpA, WbpB, WbpE, WbpD and WbpI was incubated with 0.75 mM UDP-GlcNAc, 2.0 mM NAD^+, 100 mM $(NH_4)_2SO_4$, 25 mM L-glutamate, 0.1 mM PLP, 0.75 mM AcCoA, 2.5 mM DTT, 2 mM $MgCl_2$, and 50 mM HEPES (pH 7.0) in a total reaction volume of 2 mL. The reaction was incubated at 30 °C for 8 hours, filtered, and purified by RPHPLC. Formation of the desired product was confirmed by high resolution ESI-MS and the observation of a distinct peak by CE when compared to a sample of UDP-GlcNAc(3NAc)A. WbpA and WbpI have been previously characterized and were cloned, overexpressed, and purified as described above for WbpB, WbpE, and WbpD (22,23).

RESULTS

Overexpression and Purification of WbpB, WbpE, and WbpD

All three proteins were overexpressed in high yield; 20 mg (WbpB), 110 mg (WbpE), and 15 mg (WbpD) of purified protein (> 95% purity) was routinely obtained from 1 L of cell culture. The expected molecular weights of WbpB (38,271 Da), WbpE (41,478 Da), and WbpD (23,117 Da), each containing both an N-terminal T7 and C-terminal His_6-tag, corresponded to the observed molecular weights based on SDS-PAGE (Figure 3). The identity of the proteins was further confirmed by Western blot analysis using antibodies directed against the T7 and His_6-tags. The enzymes retained activity when stored at either −20 °C (WbpB and WbpE) or 4 °C (WbpD) for a minimum of 3 months.

Functional Characterization of WbpB/WbpE by CE

Initial attempts to characterize the function of WbpB in the presence of UDP-GlcNAcA and NAD^+ or $NADP^+$ were unsuccessful despite a screen of many conditions, including addition of various monovalent and divalent cations and varying pH and temperature. However, upon the addition of WbpE and L-glutamate to the reaction, complete turnover of the UDP-GlcNAcA starting material and the formation of a new peak were observed by CE (Figure 4). The treatment of WbpE alone with UDP-GlcNAcA and obligate cofactors did not result in product formation, implying that both enzymes were required for catalysis. The product of the reaction was later identified to be UDP-GlcNAc($3NH_2$)A by mass spectrometry and NMR analysis. In addition, the use of ^{15}N-L-glutamate as the amine donor resulted in a product with an increase in mass of 1 amu, indicating that the ^{15}N-label was successfully transferred to the molecule. The coupled WbpB/WbpE reaction catalyzed product formation at a wide range of pH (5.5-10.0) and temperature (4-65 °C); however, protein precipitation and cofactor degradation were observed at both higher temperatures and alkaline pH values before complete product formation occurred. Optimal reaction conditions yielding complete conversion of starting material to product was observed at pH 8.0 and 30 °C, and have led to the generation of over 20 mg of the desired UDP-GlcNAc($3NH_2$)A in a single reaction.

α-Ketoglutarate is the Required Oxidant for NAD^+ Recycling

Further analysis of the coupled WbpB/WbpE reaction indicated that exogeneous NAD^+ or PLP was not required for product formation, suggesting that both WbpB and WbpE were purified with their respective cofactors already bound. However, the addition of 200 μM NAD^+ and 100 μM PLP to the reaction mixture aided in achieving complete turnover of substrate, which implies that the heterologously expressed proteins were not saturated with cofactor due to the limiting intracellular levels of both NAD^+ and PLP in *E. coli*. The formation of an equimolar amount of NADH was not observed in the reaction mixture, signifying that WbpB efficiently recycles the NAD^+ cofactor. In order to determine the identity of the required oxidant for NAD^+ regeneration, WbpB was incubated with UDP-GlcNAcA and 10 mM α-ketoglutarate

(α-KG). Remarkably, complete conversion of the UDP-GlcNAcA starting material to the UDP-GlcNAc(3keto)A product was observed by CE (Figure 4), whereas no turnover of UDP-GlcNAcA was seen in the absence of α-KG.

In order to determine whether α-KG was consumed by WbpB, aliquots were removed from the reaction at specific time points and reacted with *o*-phenylenediamine (OPD), which has been previously shown to selectively label α-keto acids (28,29). Analysis of the labeled aliquots by UV absorbance at 340 nm demonstrated a decrease in α-KG concentration over time, indicating that it was indeed being consumed (Figure 5). However, the use of a lower concentration of α-KG (2 mM) to maximize the observed signal decrease in the labeling reaction prevented complete turnover of the UDP-GlcNAcA starting material (70%). The product of α-KG reduction was found to be 2-hydroxyglutarate (2-HG) by thin-layer chromatography (TLC); development of TLC plates spotted with the crude reaction mixture followed by staining with either dinitrophenylhydrazine, a marker of ketones and aldehydes, or bromocresol green, specific for carboxylates, revealed the presence of a newly formed product that did not contain a ketone and ran at the same R_f value as an authentic 2-HG standard (R_f = 0.61, data not shown).

Analysis of WbpB/WbpE Specificity for Substrate

The nucleotide sugar specificity of the coupled WbpB/WbpE reaction was explored by incubating the enzymes with UDP-GlcNAc, UDP-GalNAc, and UDP-D-glucuronic acid (UDP-GlcA). No turnover was observed in the presence of UDP-GlcNAc or UDP-GalNAc, and only minimal turnover was observed (11%) when UDP-GlcA was used as the nucleotide sugar substrate. These results confirm that WbpB prefers the glucopyranose configuration of the sugar as well as the presence of both the carboxylate at the C6″ carbon and the acetylated amine at the C2″ position. As a means of analyzing the amino donor specificity of WbpE, the WbpB/WbpE coupled reaction was screened with all 20 naturally occurring L-amino acids as well as D-glutamate at a concentration of 25 mM. Other than L-glutamate, only the use of L-glutamine resulted in conversion from starting material to product (10%). This result strongly suggests that WbpE is specific for L-glutamate as the amine donor, a result that has been observed for homologous nucleotide sugar-modifying aminotransferases (32,33).

NAD^+ is the Cofactor Bound to WbpB

In order to determine whether NAD^+ or $NADP^+$ was the cofactor bound to WbpB, the enzyme was precipitated by treatment with $HClO_4$ and the pellet washed several times to recover the bound cofactor (30,31). After neutralization and lyophilization, the extract was treated with either the NAD^+-specific alcohol dehydrogenase or $NADP^+$-specific isocitrate dehydrogenase and the formation of NADH/NADPH monitored by UV at 340 nm. Upon addition of alcohol dehydrogenase, a sharp increase in absorbance was observed, indicating the presence of NAD^+ in the extract (Figure 6). Alcohol dehydrogenase is specific for NAD^+, as suggested by the lack of absorbance increase when $NADP^+$ was introduced. In addition, no absorbance increase was seen after treatment of the extract with isocitrate dehydrogenase, which serves as further evidence that the bound cofactor to WbpB is NAD^+.

Functional Characterization of WbpD by CE

Incubation of WbpD with UDP-GlcNAc($3NH_2$)A and AcCoA resulted in the complete consumption of both UDP-GlcNAc($3NH_2$)A and AcCoA and the formation of two new peaks by CE (Figure 7). Using mass spectrometry and NMR analysis, these two peaks were identified to be CoA and UDP-GlcNAc(3NAc)A. The utilization of [^{3}H]-AcCoA in the place of AcCoA resulted in [^{3}H]-labeled UDP-GlcNAc(3NAc)A, which was confirmed after purification and analysis by scintillation counting. As in the case with the WbpB/WbpE coupled reaction, WbpD was able to catalyze the acetylation of UDP-GlcNAc($3NH_2$)A at a broad range of pH

(5.5-10.0) and temperature (4-65 °C), although the optimal reaction conditions for catalysis were found to be 30 °C and pH 7.0 to limit base-promoted hydrolysis of AcCoA.

The specificity of WbpD for its nucleotide sugar substrate was investigated by incubation with UDP-GlcNAcA, UDP-GlcNAc, and UDP-2-acetamido-4-amino-2,4,6-trideoxy-D-glucosamine, the UDP-4-amino sugar product of the C4-aminotransferase from *Campylobacter jejuni*, PglE (34). No appreciable turnover of starting material was observed in any case, signifying the importance of an amine at the C3″ position for acetylation. The kinetic parameters of WbpD were determined by varying the concentration of UDP-GlcNAc($3NH_2$)A from 0.015-1.5 mM in the presence of fixed concentrations of AcCoA (1.5 mM) and WbpD. At the highest concentration of substrate, no more than 10% turnover was observed. Data were collected by manual integration of CE traces and then directly fit to the Michaelis-Menten equation using SigmaPlot (Systat Software) (Figure 8). The conclusion from this analysis is that WbpD exhibits an apparent $K_m = 107 \pm 15$ μM and $k_{cat} = (2.9 \pm 0.12) \times 10^3$ min^{-1} for its nucleotide sugar substrate, UDP-GlcNAc($3NH_2$)A.

Structural Characterization of UDP-GlcNAc($3NH_2$)A and UDP-GlcNAc(3NAc)A

NMR spectra of both UDP-GlcNAc($3NH_2$)A and UDP-GlcNAc(3NAc)A are depicted in Figure 10, and corresponding ^1H chemical shifts and coupling constants are summarized in Table 1. Proton assignments were made using COSY experiments, and HMBC and HSQC analyses were used to assign the carbon resonances. In both cases, the ^1H and ^{13}C chemical shifts of the uracil and ribose moieties matched previously published values for similar compounds (34). For both UDP-GlcNAc($3NH_2$)A and UDP-GlcNAc(3NAc)A, the $J_{1″,2″}$, $J_{2″,3″}$, $J_{3″,4″}$, and $J_{4″,5″}$ values indicate an α-glucopyranose configuration. In the ^1H spectrum of UDP-GlcNAc(3NAc)A, the presence of two singlets at 1.97 and 2.01 ppm designate that the compound is diacetylated, and the downfield shift of H-3″ from 3.57 ppm in the UDP-GlcNAc($3NH_2$)A ^1H spectrum to 4.16 ppm shows that acetylation by WbpD occurs on the 3″-amine group.

In addition to the NMR analysis, high resolution ESI-MS analysis was performed to further confirm the identity of UDP-GlcNAc($3NH_2$)A and UDP-GlcNAc(3NAc)A. This method was particularly useful due to the similarity in molecular weight of starting material (UDP-GlcNAcA, 621.34) and product (UDP-GlcNAc($3NH_2$)A, 620.35) of the coupled WbpB/WbpE reaction. The *m/z* of UDP-GlcNAc($3NH_2$)A was found to be 619.0686 $[M-H]^-$, which matched the calculated *m/z* of 619.0695 ($C_{17}H_{25}N_4O_{17}P_2^-$). In addition, ^{15}N-labeled UDP-GlcNAc($3NH_2$)A was synthesized using ^{15}N-L-glutamate as previously described and subjected to high resolution ESI-MS; the *m/z* was found to be 620.0687 ($[M-H]^-$, calculated *m/z* = 620.0666, $C_{17}H_{25}N_3{}^{15}NO_{17}P_2^-$), indicating the presence of the ^{15}N label in the nucleotide sugar structure. The *m/z* of UDP-GlcNAc(3NAc)A was experimentally determined to be 661.0790 ($[M-H]^-$, calculated *m/z* = 661.0801, $C_{19}H_{27}N_4O_{18}P_2^-$).

One-Pot Synthesis of UDP-ManNAc(3NAc)A

In order to generate UDP-ManNAc(3NAc)A in a single reaction vessel, WbpA, WbpB, WbpE, WbpD and WbpI were combined with UDP-GlcNAc and the requisite cofactors. After incubation for 8 hours, CE analysis indicated partial consumption of the UDP-GlcNAc starting material (15%) and formation of a new peak. The crude reaction mixture was purified by RP-HPLC and the identity of UDP-ManNAc(3NAc)A was confirmed by high resolution ESI-MS and comparison with a pure sample of UDPGlcNAc(3NAc)A by CE (Figure 12).

DISCUSSION

Despite the remarkable structural diversity and complexity of sugars found in nature, diacetylated aminuronic acids are quite rare. These distinctive molecules have primarily been identified in the complex cell wall matrices of pathogenic bacteria and the glycoproteins of certain archaea. To date, GlcNAc(3NAc)A has been detected in the LPS of a number of *P. aeruginosa* strains, including P1-III and P14, and the unique *N*-linked glycans of the methanogenic archaea *Methanococcus voltae* and *Methanococcus maripalidus* (35-38). In addition to *P. aeruginosa* PAO1 (serotype O5), ManNAc(3NAc)A, the C2 epimer of GlcNAc (3NAc)A, is present in the LPS of other *P. aeruginosa* strains, as well as in the cell wall polysaccharide of the gram-positive thermophile *Bacillus stearothermophilus* and the pathogens *Bordatella pertussis*, *Bordatella parapertussis* and *Bordatella bronchiseptica* (39-41). While the genes responsible for the biosynthesis of these sugars have been identified in a number of organisms, very few of the resulting proteins have been studied in biochemical detail. In this report, we describe the function of WbpB, WbpE, and WbpD, enzymes responsible for the synthesis of UDP-GlcNAc(3NAc)A in *Pseudomonas aeruginosa* PAO1. These studies complete the biochemical characterization of this critical pathway in *P. aeruginosa* and provide a means for generating UDP-GlcNAc(3NAc)A on a multimilligram scale. This rare nucleotide sugar may serve as a useful tool to unravel the complex mechanism of polysaccharide biosynthesis in related organisms.

WbpB and WbpE are a C3 dehydrogenase and aminotransferase pair responsible for the stepwise conversion of UDP-GlcNAcA to UDP-GlcNAc($3NH_2$)A. Despite screening a wide range of conditions, WbpB function was initially not observed. Only upon the addition of WbpE and L-glutamate to the reaction mixture was the complete consumption of the UDP-GlcNAcA starting material and formation of UDP-GlcNAc($3NH_2$)A detected, and further investigation showed that both enzymes were required for catalysis. The necessary coupling of dehydrogenase/aminotransferase pairs in vitro has previously been reported; for example, the GnnA and GnnB enzymes from the gram-negative acidophile *Acidithiobacillus ferrooxidans* must both be present to observe the conversion of UDP-GlcNAc to the corresponding C3-modified UDP-GlcNAc($3NH_2$) (42). Interestingly, unlike other dehydrogenase/aminostransferase pairs, the coupled WbpB/WbpE reaction did not require exogeneous NAD^+ for product formation, suggesting that the cofactor is efficiently recycled by WbpB throughout the course of the reaction. Efforts to determine the required oxidant responsible for NAD^+ regeneration revealed that addition of α-KG, produced by WbpE from L-glutamate, to the WbpB reaction is sufficient for catalysis of substrate to product. Using a combination of α-KG labeling studies and thin-layer chromatography, we have demonstrated that α-KG is consumed over the course of the WbpB reaction and that the product of α-KG reduction is 2-HG. We therefore conclude that the required pairing of WbpB and WbpE is driven by the use of α-KG as the critical oxidant for NAD^+ regeneration by WbpB. While the concomitant reduction of α-KG and oxidation of NADH has been previously observed in nature, such as in the case of SerA 3-phosphoglycerate dehydrogenase (43), to our knowledge this is the first reported evidence of α-KG shunting in a nucleotide-sugar biosynthesis pathway, thus representing a novel method of NAD^+ recycling.

A close comparison of the structures of UDP-GlcNAc(3keto)A and α-KG offers insight into a possible pathway for the recycling of NAD^+. As depicted in Figure 13, the terminal carboxylate, carbon backbone and ketone of both molecules spatially overlap, suggesting similar binding interactions within the active site. One may envision a catalytic cycle in which initially, UDP-GlcNAcA is converted to UDP-GlcNAc(3keto)A, resulting in reduction of NAD^+ to NADH. After dissociation of UDP-GlcNAc(3keto)A, a molecule of α-KG enters the active site and is positioned favorably to permit formation of 2-HG and the oxidation of NADH back to NAD^+, both completing the NAD^+ regeneration cycle and preparing WbpB for catalysis of

another molecule of UDP-GlcNAcA. The underlying necessity for the coupled activities of the dehydrogenase WbpB and aminotransferase WbpE remains unclear. One hypothesis is that UDPGlcNAc(3keto)A is labile at physiological conditions, and thus the pairing of WbpB and WbpE activities allows for the direct transfer of the ketone intermediate from WbpB to WbpE. However, the observation of WbpB function in the presence of α-KG implies that there is no required physical interaction between WbpB and WbpE. After the review of this report, a preliminary study from the Lam group on this biosynthetic pathway appeared in press. This study described the required coupling of WbpB and WbpE for function; however, it unfortunately provides no information about cofactor requirements and failed to observe the α-KG-dependent dehydrogenase activity of WbpB in the absence of WbpE, instead attributing the pairing of WbpB and WbpE to a necessary physical interaction alone (44). Investigations are currently underway in our laboratory to further characterize the coupling of WbpB and WbpE as well as the potential applications of the UDP-GlcNAc(3keto)A intermediate.

The next enzyme in the UDP-ManNAc(3NAc)A biosynthetic pathway, WbpD, catalyzes the AcCoA-dependent acetylation of UDP-GlcNAc(3NH_2)A to give UDP-GlcNAc(3NAc)A. Earlier analysis of WbpD showed that it exhibits left-handed β-helical (LbH) structure and thus is a member of the hexapeptide acyltransferase superfamily (21,45). Enzymes in this class of acyland acetyltransferases include the lipid A acyltransferase LpxA, the glucosamine 1-phosphate *N*-acetyltransferase GlmU and the UDP-4-amino acetyltransferase PglD, all of which contain numerous repeats of the hexapeptide motif L/I/V-[G/A/E/D]-X_4-[L/I/V] similar to WbpD (46-48). Based on the derived kinetic parameters in this study, WbpD has a greater affinity for its nucleotide sugar substrate UDP-GlcNAc(3NH_2)A (apparent K_m = 107 ± 16 μM) and catalyzes acetylation in a moderately rapid fashion (k_{cat} = 2.9 ± 0.12 × 10^3 min^{-1}) when compared with PglD, the C4 acetyltransferase involved in the biosynthesis of UDP-*N*,*N*′-diacetylbacillosamine from *Campylobacter jejuni* characterized previously (K_m = 410 ± 78 μM and k_{cat} = 4.83 ± 0.30 × 10^5 min^{-1}) (49). PglD is a highly efficient enzyme (k_{cat}/K_m = 1.18 × 10^6 min^{-1} mM^{-1}), and it is hypothesized that its ability to rapidly carry out acetylation serves to prevent the buildup of early intermediates produced by the slower preceding enzymes (PglE and PglF) in the biosynthetic sequence. While the kinetic parameters of WbpB and WbpE have yet to be determined, it is clear that WbpD (k_{cat}/K_m = 2.69 × 10^4 min^{-1} mM^{-1}) is in fact more efficient than WbpA (k_{cat}/K_m = 913 min^{-1} mM^{-1}), the first enzyme in the pathway, in turning over its nucleotide sugar substrate (22); perhaps the increased efficiency of WbpD provides the same function in this case as well.

We have shown that by combining WbpA, WbpB, WbpE, WbpD and WbpI with UDPGlcNAc and obligate cofactors and substrates in vitro, it is possible to generate UDPManNAc(3NAc)A in a one-pot reaction. This is a common feature of many stepwise biosynthetic pathways, as exemplified by the Pgl pathway responsible for *N*-linked glycosylation in *Campylobacter jejuni* (49). This one-pot biotransformation now provides a platform for screening the entire sequence of enzymes for possible inhibitors in a high-throughput manner.

In conclusion, this report describes the biochemical characterization of WbpB, WbpE, and WbpD, three key enzymes responsible for the formation of UDP-GlcNAc(3NAc)A. It provides a facile route to the chemoenzymatic synthesis of milligram quantities of this rare nucleotide sugar and completes the annotation of the UDP-ManNAc(3NAc)A biosynthetic pathway in *P. aeruginosa*. Due to the presence of UDP-GlcNAc(3NAc)A and UDP-ManNAc(3NAc)A in related pathogens, we envision that the methods outlined herein may provide useful tools to probe similar biosynthetic pathways in these organisms. Lastly, as these enzymes play a critical role in the formation of lipopolysaccharide, they may present new targets for the development of potential therapeutics for treatment of *P. aeruginosa* infection.

Supplementary Material

Refer to Web version on PubMed Central for supplementary material.

ACKNOWLEDGMENT

We are grateful to Dr. Nelson Olivier for technical advice and members of the Imperiali laboratory for helpful discussions and critical reading of this manuscript. We thank Dr. Jeff Simpson of the MIT Department of Chemistry Instrumentation Facility for assistance with NMR acquisition.

REFERENCES

1. Pier GB. *Pseudomonas aeruginosa* lipopolysaccharide: A major virulence factor, initiator of inflammation and target for effective immunity. Int. J. Med. Microbiol 2007;297:277–295. [PubMed: 17466590]
2. Neu HC. Infections due to gram-negative bacteria: An overview. Rev. Infect. Dis 1985;7:S778–S782. [PubMed: 3909337]
3. Diaz MH, Shaver CM, King JD, Musunuri S, Kazzaz JA, Hauser AR. *Pseudomonas aeruginosa* induces localized immunosuppression during pneumonia. Infect. Immun 2008;76:4414–4421. [PubMed: 18663007]
4. Tang HB, DiMango E, Bryan R, Gambello M, Iglewski BH, Goldberg JB, Prince A. Contribution of specific *Pseudomonas aeruginosa* virulence factors to pathogenesis of pneumonia in a neonatal mouse model of infection. Infect. Immun 1996;64:37–43. [PubMed: 8557368]
5. Son MS, Matthews WJ Jr. Kang Y, Nguyen DT, Hoang TT. In vivo evidence of *Pseudomonas aeruginosa* nutrient acquisition and pathogenesis in the lungs of cystic fibrosis patients. Infect. Immun 2007;75:5313–5324. [PubMed: 17724070]
6. Hancock RE. Resistance mechanisms in *Pseudomonas aeruginosa* and other nonfermative gram-negative bacteria. Clin. Infect. Dis 1998;27:S93–S99. [PubMed: 9710677]
7. Mesaros N, Nordmann P, Plesiat P, Roussel-Delvallez M, Van Eldere J, Y. G, Van Laethem Y, Jacobs F, Lebecque P, Malfroot A, Tulkens PM, Van Bambeke F. *Pseudomonas aeruginosa*: resistance and therapeutic options at the turn of the new millennium. Clin. Microbiol. Infect 2007;13:560–578. [PubMed: 17266725]
8. Zaborina O, Holbrook C, Chen Y, Long J, Zaborin A, Morozova I, Fernandez H, Wang Y, Turner JR, Alverdy JC. Structure-function aspects of PstS in multi-drug resistant *Pseudomonas aeruginosa*. PLoS Pathog 2008;4:e43. [PubMed: 18282104]
9. Döring G, Pier GB. Vaccines and immunotherapy against *Pseudomonas aeruginosa*. Vaccine 2008;26:1011–1024. [PubMed: 18242792]
10. Cryz SJ Jr. Pitt TL, Furer E, Germanier R. Role of lipopolysaccharide in virulence of *Pseudomonas aeruginosa*. Infect. Immun 1984;44:508–513. [PubMed: 6425224]
11. Lam MY, McGroarty EJ, Kropinski AM, MacDonald LA, Pedersen SS, Hoiby N, Lam JS. Occurrence of a common lipopolysaccharide antigen in standard and clinical strains of *Pseudomonas aeruginosa*. J. Clin. Microbiol 1989;27:962–967. [PubMed: 2501356]
12. Rocchetta HL, Burrows LL, Lam JS. Genetics of O-antigen biosynthesis in *Pseudomonas aeruginosa*. Microbiol. Mol. Biol. Rev 1999;63:523–553. [PubMed: 10477307]
13. Knirel YA, Bystrova OV, Kocharova NA, Zahringer U, Pier GB. Conserved and variable structural features in the lipopolysaccharide of *Pseudomonas aeruginosa*. J. Endotoxin Res 2006;12:324–336. [PubMed: 17254386]
14. Knirel YA, Vinogradov EV, Kocharova NA, Paramonov NK, Kochetkov NK, Dmitriev BA, Stanislavsky ES, Lanyi B. The structure of O-specific polysaccharides and serological classification of *Pseudomonas aeruginosa*. Acta Microbiol. Hung 1988;35:3–24. [PubMed: 3134788]
15. Bystrova OV, Knirel YA, Lindner B, Kocharova NA, Kondakova AN, Zahringer U, Pier GB. Structures of the core oligosaccharide and O-units in the R- and SR-type lipopolysaccharides of reference strains of *Pseudomonas aeruginosa* O-serogroups. FEMS Immunol. Med. Microbiol 2006;46:85–99. [PubMed: 16420601]

16. Arsenault TL, Hughes DW, MacLean DB, Szarek W, Kropinkski AMB, Lam JS. Structural studies on the polysaccharide portion of "A-band" lipopolysaccharide from a mutant (AK1401) of *Pseudomonas aeruginosa* strain PAO1. Can. J. Chem 1991;69:1273–1280.

17. Dasgupta T, de Kievit TR, Masoud H, Altman E, Richards JC, Sadovskaya I, Speert DP, Lam JS. Characterization of lipopolysaccharide-deficient mutants of *Pseudomonas aeruginosa* derived from serotypes O3, O5, and O6. Infect. Immun 1994;62:809–817. [PubMed: 8112851]

18. Hancock RE, Mutharia LM, Chan L, Darveau RP, Speert DP, Pier GB. *Pseudomonas aeruginosa* isolates from patients with cystic fibrosis: a class of serum-sensitive, nontypable strains deficient in lipopolysaccharide O side chains. Infect. Immun 1983;42:170–177. [PubMed: 6413410]

19. Kochetkov NK, Knirel YA. Structure of lipopolysaccharides from gram-negative bacteria. III. Structure of O-specific polysaccharides. Biochemistry (Moscow) 1994;59:1325–1383.

20. Burrows LL, Charter DF, Lam JS. Molecular characterization of the *Pseudomonas aeruginosa* serotype O5 (PAO1) B-band lipopolysaccharide gene cluster. Mol. Microbiol 1996;22:481–495. [PubMed: 8939432]

21. Wenzel CQ, Daniels C, Keates RAB, Brewer D, Lam JS. Evidence that WbpD is an *N*-acetyltransferase belonging to the hexapeptide acyltransferase superfamily and an important protein for O-antigen biosynthesis in *Pseudomonas aeruginosa* PAO1. Mol. Microbiol 2005;57:1288–1303. [PubMed: 16102001]

22. Miller WL, Wenzel CQ, Daniels C, Larocque S, Brisson J-R, Lam JS. Biochemical characterization of WbpA, a UDP-*N*-acetyl-d-glucosamine 6-dehydrogenase involved in O-antigen biosynthesis in *Pseudomonas aeruginosa* PAO1. J. Biol. Chem 2004;279:37551–37558. [PubMed: 15226302]

23. Westman EL, McNally DJ, Rejzek M, Miller WL, Kannathasan VS, Preston A, Maskell DJ, Field RA, Brisson J-R, Lam JS. Identification and biochemical characterization of two novel UDP-2,3-diacetamido-2,3-dideoxy-α-d-glucuronic acid 2-epimerases from respiratory pathogens. Biochem. J 2007;405:123–130. [PubMed: 17346239]

24. Westman EL, Preston A, Field RA, Lam JS. Biosynthesis of a rare di-*N*-acetylated sugar in the lipopolysaccharides of both *Pseudomonas aeruginosa* and *Bordetella pertussis* occurs via an identical scheme despite different gene clusters. J. Bacteriol 2008;190:6060–6069. [PubMed: 18621892]

25. Burrows LL, Pigeon KE, Lam JS. *Pseudomonas aeruginosa* B-band lipopolysaccharide genes wbpA and wbpI and their *Escherichia coli* homologues wecC and wecB are not functionally interchangeable. FEMS Microbiol. Lett 2000;189:135–141. [PubMed: 10930727]

26. Rejzek M, Mukhopadhyay B, Wenzel CQ, Lam JS, Field RA. Direct oxidation of sugar nucleotides to the corresponding uronic acids: TEMPO and platinum-based procedures. Carb. Res 2007;342:460–466.

27. Stahl, E. Thin-Layer Chromatography: A Laboratory Handbook. Vol. 2nd ed.. New York; Springer-Verlag: 1969.

28. Lanning MC, Cohen SS. The detection and estimation of 2-ketohexonic acids. J. Biol. Chem 1951;189:109–114. [PubMed: 14832222]

29. Kalliri E, Mulrooney SB, Hausinger RP. Identification of *Escherichia coli* YgaF as an l-2-hydroxyglutarate oxidase. J. Bacteriol 2008;190:3793–3798. [PubMed: 18390652]

30. Ni Y, McPhie P, Deacon A, Ealick S, Coleman WG Jr. Evidence that $NADP^+$ is the physiological cofactor of ADP-l-glycero-d-mannoheptose 6-epimerase. J. Biol. Chem 2001;276:27329–27334. [PubMed: 11313358]

31. Klepp J, Retey J. The stoichiometry of the tightly bound NAD^+ in urocanase: Separation and characterization of fully active and inhibited forms of the enzyme. Eur. J. Biochem 1989;185:615–619. [PubMed: 2574107]

32. Obhi RK, Creuzenet C. Biochemical characterization of the *Campylobacter jejuni* Cj1294, a novel UDP-4-keto-6-deoxy-GlcNAc aminotransferase that generates UDP-4-amino-4,6-dideoxy-GalNAc. J. Biol. Chem 2005;280:20902–20908. [PubMed: 15790564]

33. Vijayakumar S, Merkx-Jacques A, Ratnayake DB, Gryski I, Obhi RK, Houle S, Dozois CM, Creuzenet C. Cj1121c, a novel UDP-4-keto-6-deoxy-GlcNAc C-4 aminotransferase essential for protein glycosylation and virulence in *Campylobacter jejuni*. J. Biol. Chem 2006;281:27733–27743. [PubMed: 16690622]

34. Schoenhofen IC, McNally DJ, Vinogradov E, Whitfield D, Young NM, Dick S, Wakarchuk WW, Brisson J-R, Logan SM. Functional characterization of dehydratase/aminotransferase pairs from *Helicobacter* and *Campylobacter*: Enzymes distinguishing the pseudaminic acid and bacillosamine biosynthetic pathways. J. Biol. Chem 2006;281:723–732. [PubMed: 16286454]
35. Knirel YA, Kochetkov NK. 2,3-Diamino-2,3-dideoxyuronic and 5,7-diamino-3,5,7,9-tetradeoxynonulosonic acids: new components of bacterial polysaccharides. FEMS Microbiol. Rev 1987;46:381–385.
36. Okuda S, Murata S, Suzuki N. Isolation and identification of uridine(5′)-diphospho(1)-2,3-diacetamido-2,3-dideoxy-alpha-d-glucopyranuronic acid from *Pseudomonas aeruginosa* P1-III. Biochem. J 1986;239:733–738. [PubMed: 3030271]
37. Voisin S, Houliston RS, Kelly J, Brisson J-R, Watson D, Bardy SL, Jarrell KF, Logan SM. Identification and characterization of the unique *N*-linked glycan common to the flagellins and S-layer glycoprotein of *Methanococcus voltae*. J. Biol. Chem 2005;280:16586–16593. [PubMed: 15723834]
38. Kelly J, Logan SM, Jarrell KF, VanDyke DJ, Vinogradov EV. A novel *N*-linked flagellar glycan from *Methanococcus maripalidus*. Carb. Res 2009;344:648–653.
39. Shaffer C, Kahlig H, Christian R, Schulz G, Zanyi S, Messner P. The diacetamidodideoxyuronic-acid-containing glycan chain of *Bacillus stearothermophilus* NRS 2004/3a represents the secondary cell-wall polymer of wild-type *B. stearothermophilus* strains. Microbiol 1999;145:1575–1583.
40. Allen A, Maskell D. The identification, cloning and mutagenesis of a genetic locus required for lipopolysaccharide biosynthesis in *Bordatella pertussis*. Mol. Microbiol 1996;19:37–52. [PubMed: 8821935]
41. Caroff M, Brisson J-R, Martin A, Karibian D. Structure of the *Bordetella pertussis* 1414 endotoxin. FEBS Lett 2000;477:8–14. [PubMed: 10899302]
42. Sweet CR, Ribeiro AA, Raetz CRH. Oxidation and transamination of the 3″-position of UDP-*N*-acetylglucosamine by enzymes from *Acidithiobacillus ferrooxidans*: Role in the formation of lipid A molecules with four amide-linked acyl chains. J. Biol. Chem 2004;279:25400–25410. [PubMed: 15044494]
43. Zhao G, Winkler ME. A novel α-ketoglutarate reductase activity of the *serA*-encoded 3-phosphoglycerate dehydrogenase of *Escherichia coli* K-12 and its possible implications for human 2-hydroxyglutaric adicuria. J. Bacteriol 1996;178:232–239. [PubMed: 8550422]
44. Westman EL, McNally DJ, Charchoglyan A, Brewer D, Field RA, Lam JS. Characterization of WbpB, WbpE, and WbpD, and reconstitution of a pathway for the biosynthesis of UDP-2,3-diacetamido-2,3-dideoxy-D-mannuronic acid in *Pseudomonas aeruginosa*. J. Biol. Chem. 2009[Online early access]. DOI:10.1074/jbc.M808583200
45. Raetz CRH, Roderick SL. A left-handed parallel β-helix in the structure of UDP-*N*-acetylglucosamine acyltransferase. Science 1995;270:997–1000. [PubMed: 7481807]
46. Vuorio R, Härkönen T, Tolvanen M, Vaara M. The novel hexapeptide motif found in the acyltransferases LpxA and LpxD of lipid A biosynthesis is conserved in various bacteria. FEBS Lett 1994;337:289–292. [PubMed: 8293817]
47. Olsen LR, Vetting MW, Roderick SL. Structure of the *E. coli* bifunctional GlmU acetyltransferase active site with substrates and products. Protein Sci 2007;16:1230–1235. [PubMed: 17473010]
48. Olivier NB, Imperiali B. Crystal structure and catalytic mechanism of PglD from *Campylobacter jejuni*. J. Biol. Chem 2008;283:27937–27946. [PubMed: 18667421]
49. Olivier NB, Chen MM, Behr JR, Imperiali B. In vitro biosynthesis of UDP-*N*,*N*′-diacetylbacillosamine by enzymes of the *Campylobacter jejuni* general protein glycosylation system. Biochemistry 2006;45:13659–13669. [PubMed: 17087520]

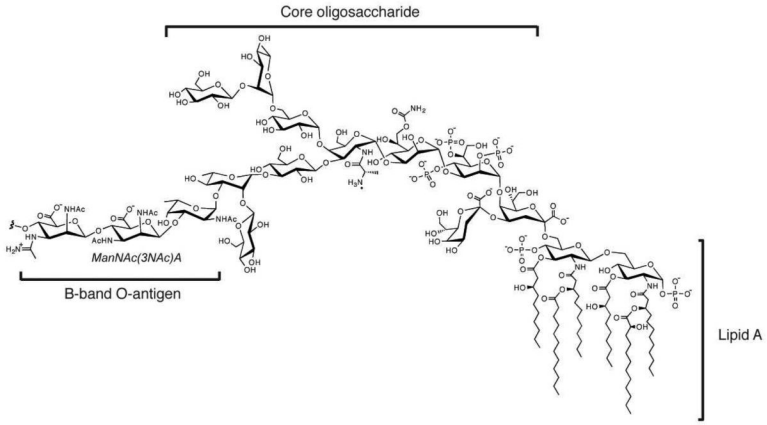

Figure 1.
General structure of the lipopolysaccharide of *P. aeruginosa* PAO1 (serotype O5), depicted with one unit of the B-band form of O-antigen.

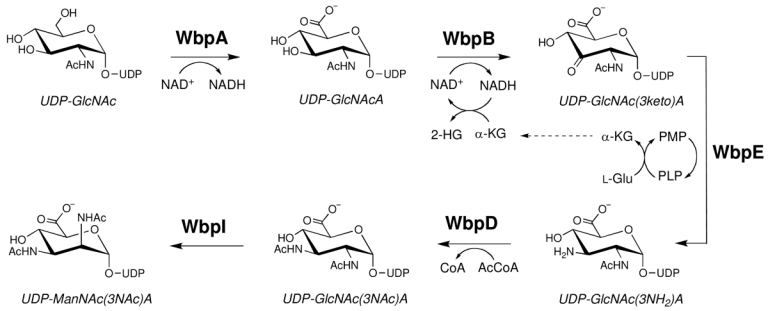

Figure 2.

Biosynthetic pathway of UDP-ManNAc(3NAc)A in *P. aeruginosa* PAO1. Abbreviations: AcCoA, acetyl-coenzyme A; CoA, coenzyme A, 2-HG, 2-hydroxyglutarate; α-KG, α-ketoglutarate; NAD^+, nicotinamide adenine dinucleotide; NADH, nicotinamide adenine dinucleotide hydrate; PLP, pyridoxal 5′-phosphate; PMP, pyridoxamine 5′phosphate.

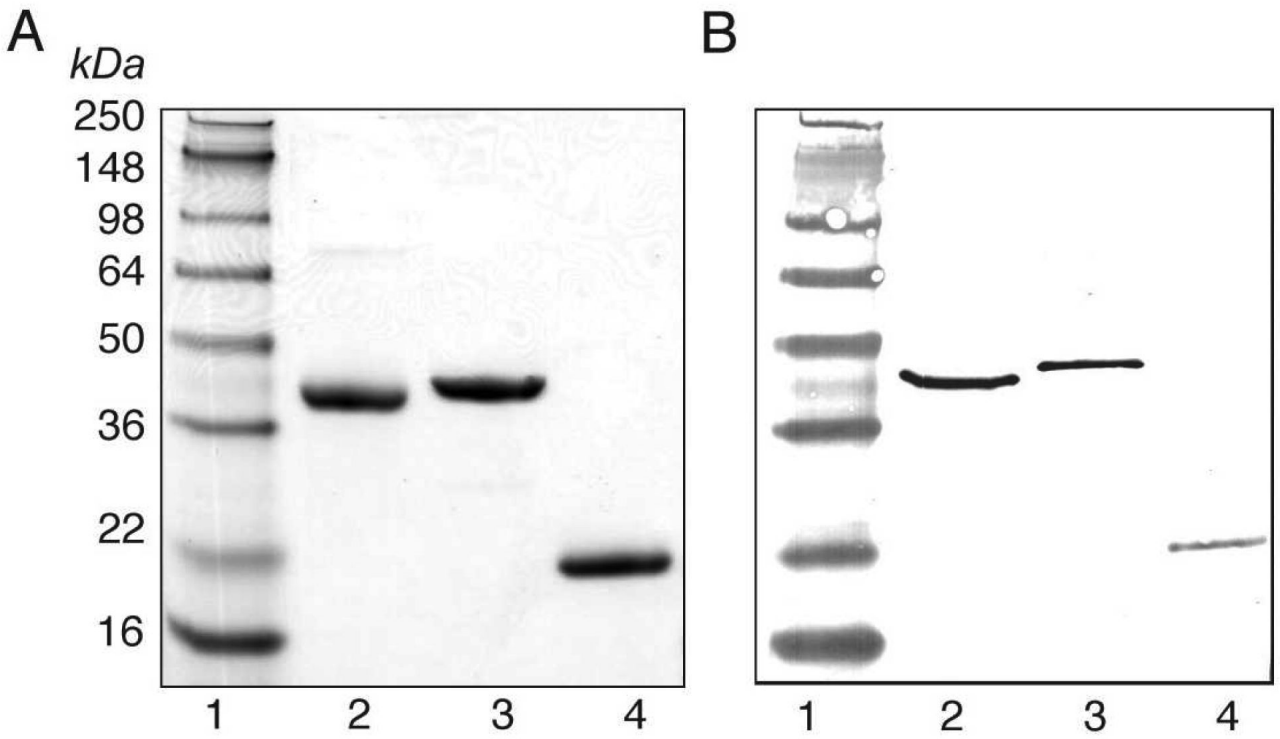

Figure 3.
(A) 10-20% gradient SDS-PAGE and (B) Anti-T7 Western blot. (1) MW standard; (2) WbpB; (3) WbpE; (4) WbpD

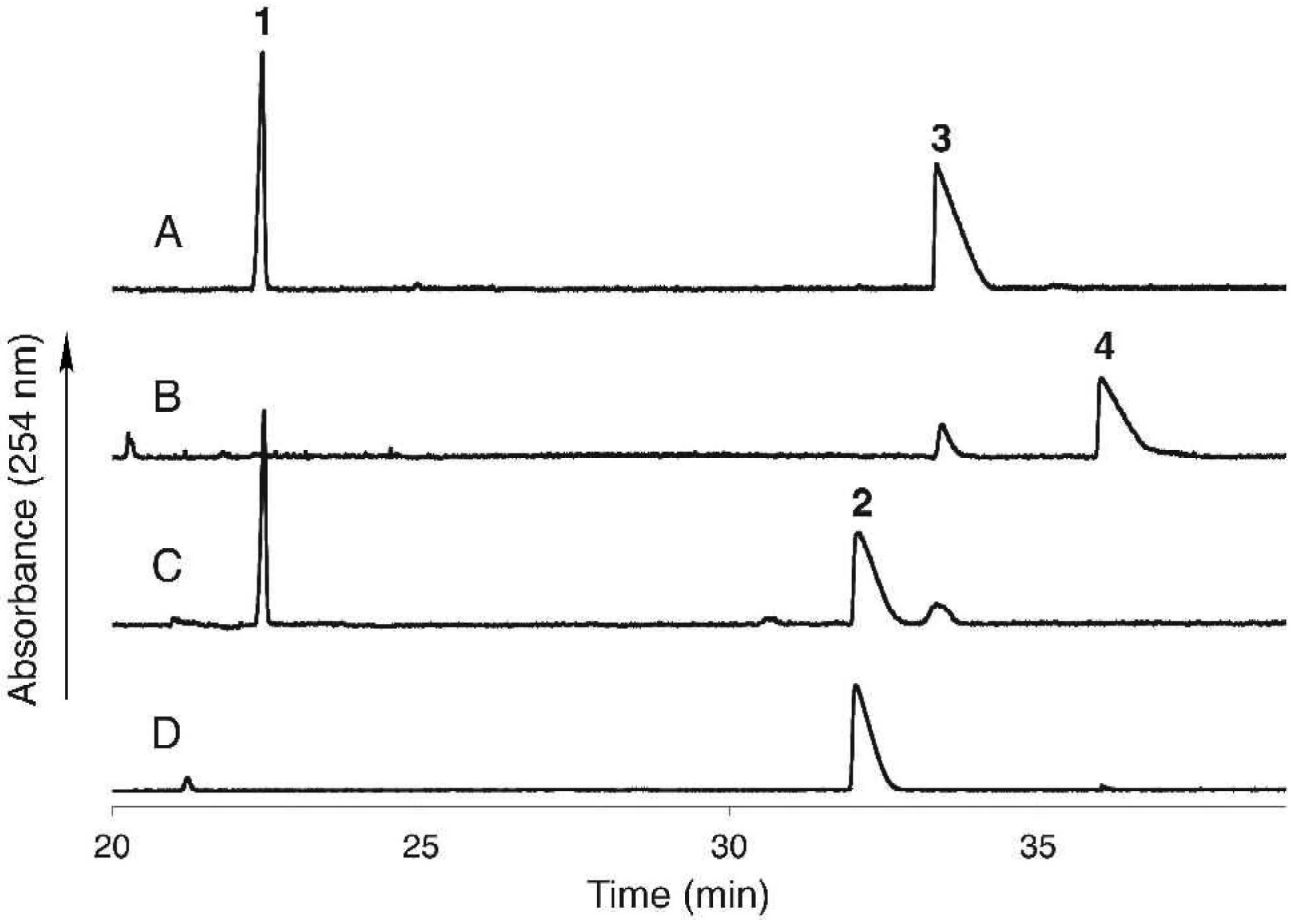

Figure 4.

Capillary electrophoresis chromatogram representing (A) WbpB reaction in the absence of α-KG, indicating no substrate conversion, (B) WbpB reaction containing 10 mM α-KG, depicting consumption of UDP-GlcNAcA, (C) crude coupled WbpB/WbpE reaction, (D) pure UDP-GlcNAc($3NH_2$)A. (1) NAD^+; (2) UDP-GlcNAc($3NH_2$)A; (3) UDP-GlcNAcA; (4) UDP-GlcNAc(3keto)A.

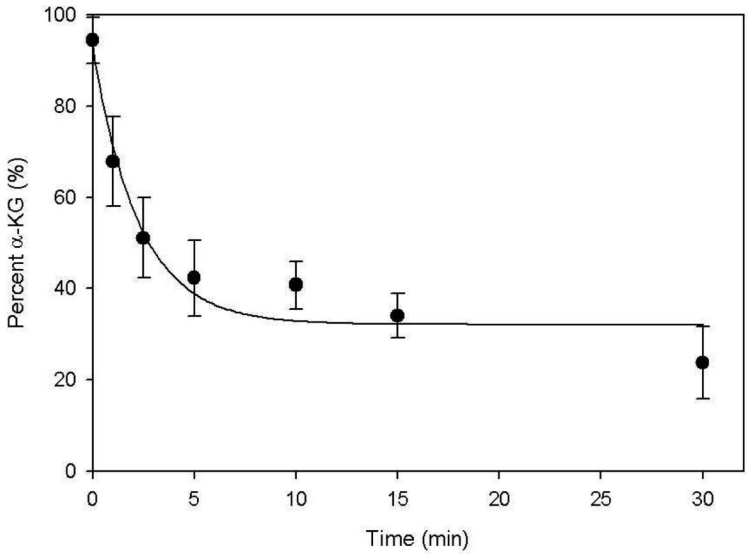

Figure 5.

Verification of α-KG consumption over the course of the WbpB reaction, indicating it is the required oxidant for NAD^+ recycling. The reaction contained 0.75 mM UDP-GlcNAcA, 50 mM HEPES (pH 8.0), 2 mM α-KG and 2.5 g WbpB. Aliquots were removed from the reaction at selected time points, quenched, labeled with OPD, and analyzed by absorbance at 340 nm. Data represent the average of three experiments.

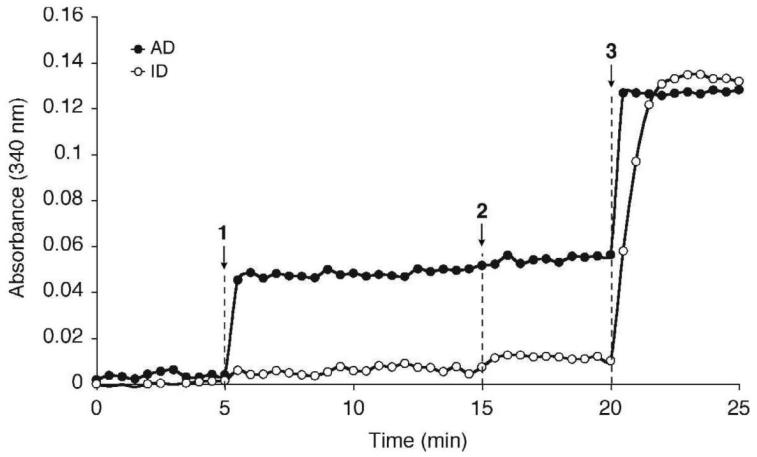

Figure 6.

Identification of NAD^+ as the bound cofactor to WbpB by UV analysis. WbpB extract was treated with either NAD-dependent alcohol dehydrogenase (AD) or NADP-dependent isocitrate dehydrogrenase (ID) and analyzed for the formation of NADH/NADPH by absorbance at 340 nm. (1) Enzyme added to extract in cuvette; (2) $NADP^+$ (AD) or NAD^+ (ID) added to reaction to address specificity; (3) NAD^+ (AD) or $NADP^+$ (ID) added to reaction to check for activity.

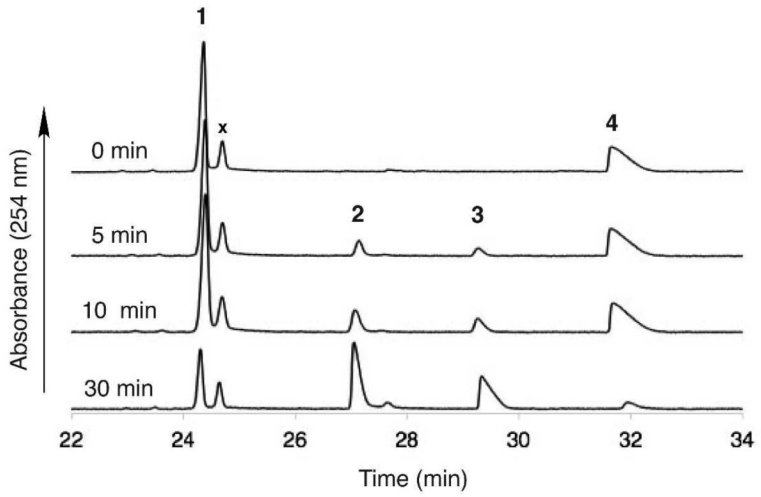

Figure 7.

CE time course analysis of the WbpD reaction. (1) AcCoA; (2) CoA; (3) UDPGlcNAc(3NAc)A; (4) UDP-GlcNAc(3NH_2)A. The peak labeled **x** represents an impurity present in the AcCoA starting material.

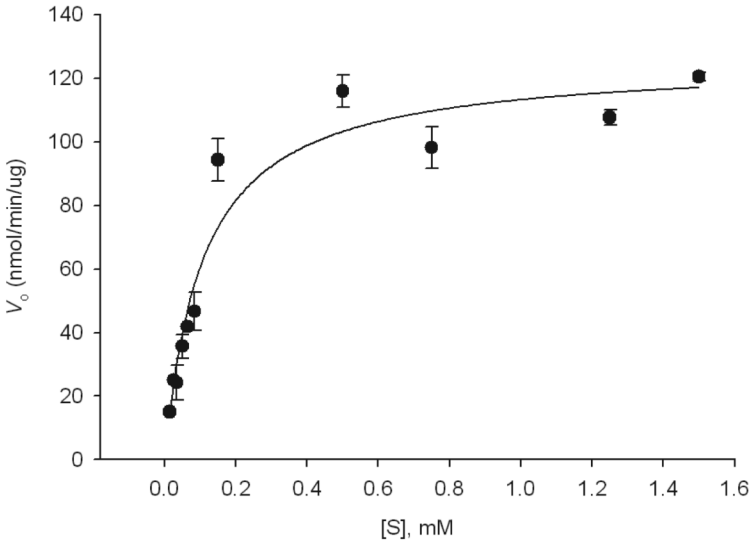

Figure 8.

Michaelis-Menten diagram depicting WbpD kinetic parameters. Reactions were carried out 50 mM HEPES, pH 7.0 at 30 °C using 0.5 ng WbpD, with AcCoA as the fixed substrate (1.5 mM) and UDP-GlcNAc(3NH_2)A as the variable substrate (0.015-1.5 mM).

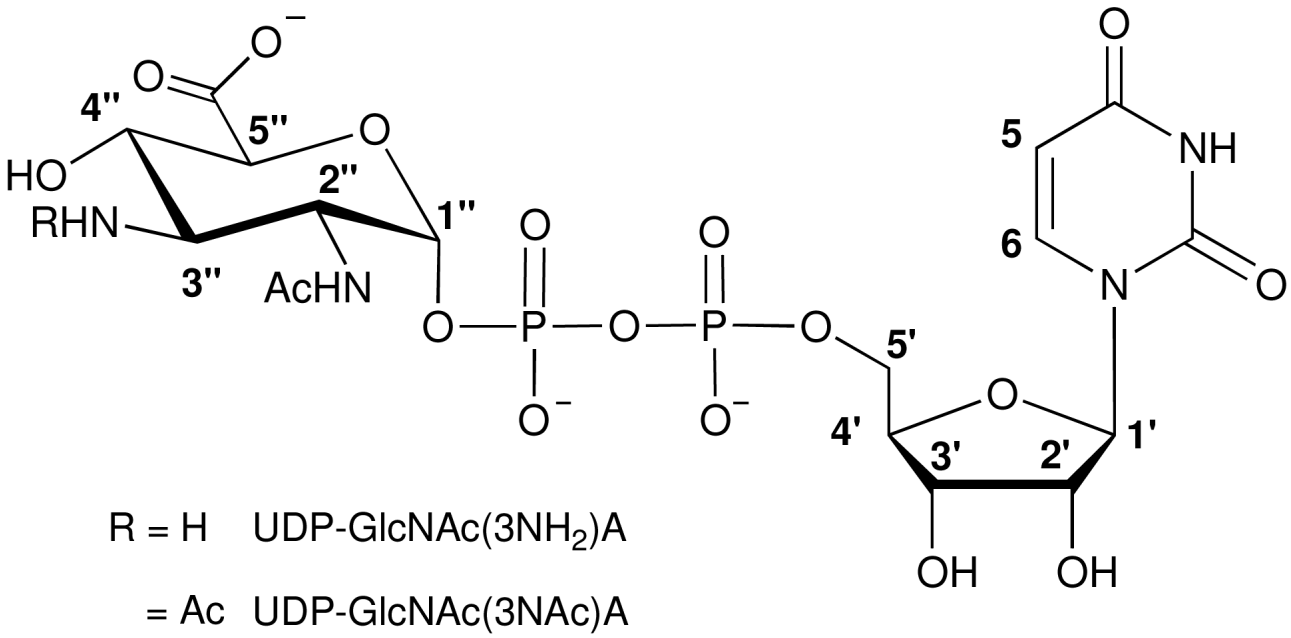

Figure 9.
Structures of UDP-GlcNAc($3NH_2$)A and UDP-GlcNAc(3NAc)A.

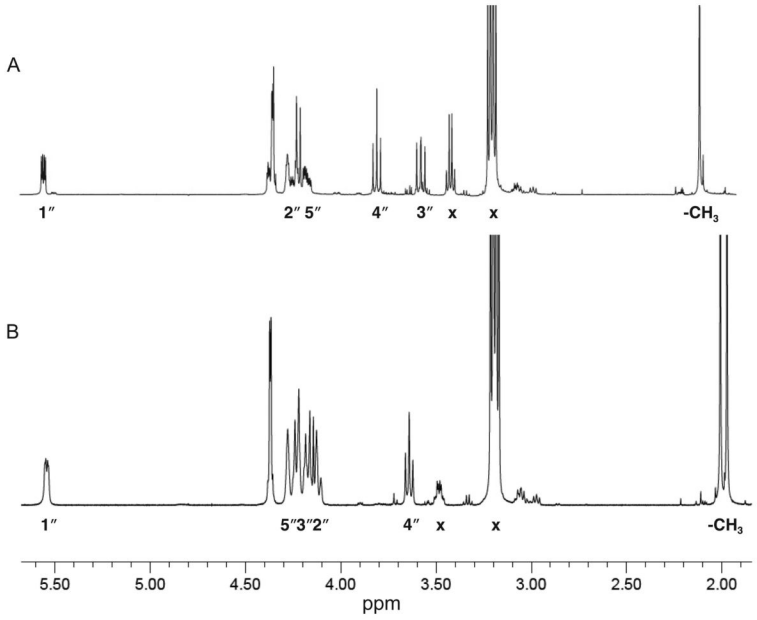

Figure 10.

Partial ^{1}H spectra of (A) UDP-GlcNAc(3NH_2)A and (B) UDP-GlcNAc(3NAc)A. Protons corresponding to the glucopyranose moiety are labeled. Spectra were acquired at 25 °C with suppression of the HOD signal at 4.80 ppm. Peaks labeled with **x** indicate impurities from residual triethylamine.

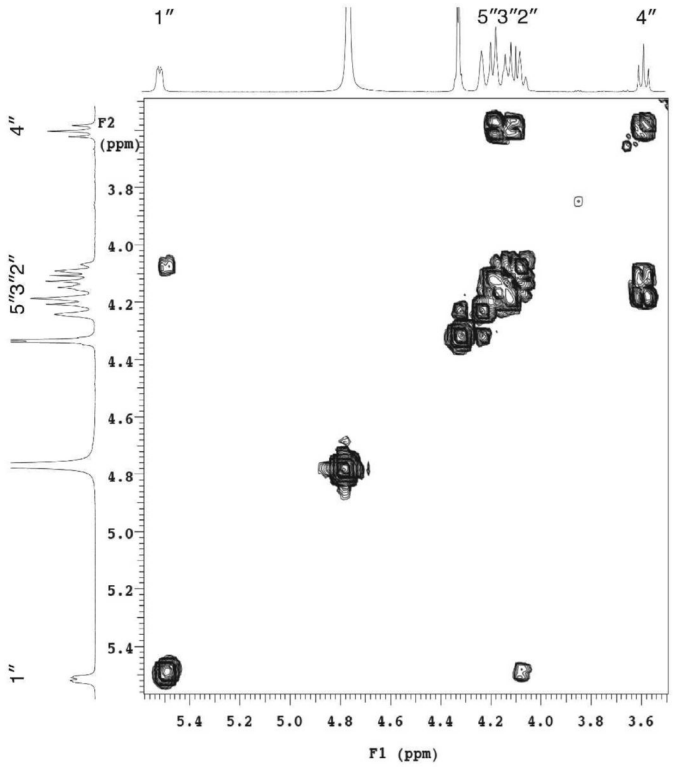

Figure 11.
Partial two-dimensional COSY spectrum of UDP-GlcNAc(3NAc)A. The spectrum was recorded at 25 °C and is expanded to highlight the glucopyranose resonances.

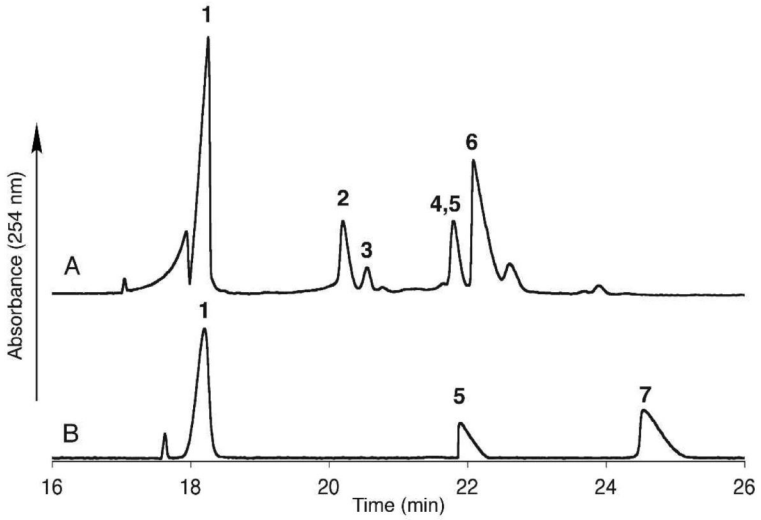

Figure 12.

CE analysis of the (A) crude one-pot reaction of WbpA, WbpB, WbpE, WbpD and WbpI and (B) purified UDP-ManNAc(3NAc)A, with both NAD^+ and UDP-GlcNAc(3NAc)A included as references. UDP-ManNAc(3NAc)A has the same retention time as NADH. (1) NAD^+; (2) UDP-GlcNAc; (3) AcCoA; (4) NADH; (5) UDP-ManNAc(3NAc)A; (6) CoA; (7) UDP-GlcNAc(3NAc)A.

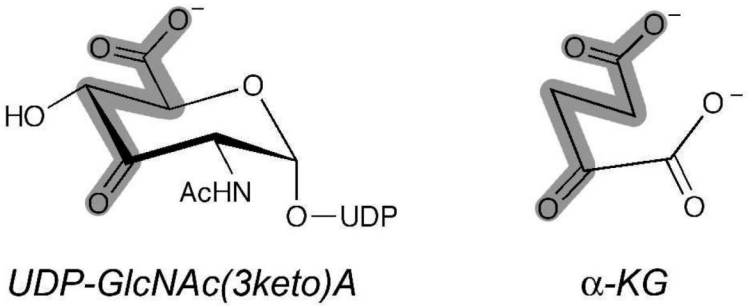

Figure 13.
Comparison of UDP-GlcNAc(3keto)A and α-KG structures, suggesting a similar binding orientation of the carboxylate and ketone moieties in the WbpB active site.

Table 1

^{1}H Chemical Shifts and Coupling Constant Assignments

Moiety	UDP-GlcNAc(3NH$_2$)A			UDP-GlcNAc(3NAc)A		
	δ_H (ppm)	***J***	**Hz**	**δ_H (ppm)**	***J***	**Hz**
Uracil						
H-5	5.95	$J_{5,6}$	8.1	5.96	$J_{5,6}$	8.1
H-6	7.94			7.95		
Ribose						
H-1′	5.97	$J_{1',2}$	4.4	5.99	$J_{1',2}$	4.4
H-2′	4.36			4.37		
H-3′	4.36			4.37		
H-4′	4.29			4.29		
H-5′a	4.17	$J_{5'a,5'b}$	11.7	4.19	$J_{5'a,5'b}$	11.2
H-5′b	4.23			4.24		
Pyranose						
H-1″	5.57	$J_{1'',P}$	7.4	5.54	$J_{1'',P}$	7.1
		$J_{1'',2''}$	3.2		$J_{1'',2''}$	2.7
H-2″	4.32	$J_{2'',3''}$	11.0	4.13	$J_{2'',3''}$	~9.5
H-3″	3.57	$J_{3'',4''}$	10.0	4.16	$J_{3'',4''}$	9.8
H-4″	3.80	$J_{4'',5''}$	10.1	3.64	$J_{4'',5''}$	9.8
H-5″	4.19			4.24		
Acetyl	2.09			2.00		
				1.97		